ELSEVIER

Chemical Engineering Journal 83 (2001) 45–53

Chemical Engineering Journal

www.elsevier.com/locate/cej

Short communication

A study of bubbly flow using resistivity probes in a novel configuration

K. Sanaullah [a], S.H. Zaidi [b], J.H. Hills [a,*]

[a] *Department of Mechanical Engineering, University of Nottingham, Nottingham NG7 2RD, UK*
[b] *School of Chemical, Environmental and Mining Engineering, University of Nottingham, Nottingham NG7 2RD, UK*

Received 12 September 1999; received in revised form 26 June 2000; accepted 26 June 2000

Abstract

Among the various methods used for bubbly flow measurements, the double-sensor resistivity probe has been found very effective. Resistivity probes in horizontal and vertical configurations suffer from problems of stability and hydrodynamic resistance, respectively. Better results can be obtained by using an inclined probe. The impact of inclination on the measured bubble size, bubble frequency, local void fraction and interfacial area density concentration has been investigated in this study. For this purpose data from two inclined probes (110° and 145°) has been compared with that from a vertical probe. All three probes were used in a 150 mm diameter flow column. The flow conditions were chosen to develop a discrete two-phase bubbly flow. It was found that probe inclination could have a great effect on the fraction of bubbles captured by both probes, but that the effect on the various measured parameters was less. Among the three probes, the 110° inclined probe gave the best performance.

Keywords: Bubbly flow; Resistivity; Novel configuration; Needle probes

1. Introduction

Two-phase gas–liquid flow occurs widely in many applications in the chemical, mechanical, gas and petroleum and nuclear industries. The interface between two fluids is very complex and can assume different shapes or patterns, which have been categorized into five main regimes for vertical upflow. These regimes, which include bubbly flow, slug flow, churn flow and annular flow, depend on the flow rates of each phase involved, the physical properties of the fluids and the flow geometry.

Slug flow is undesirable, and so several researchers have investigated the bubble-to-slug flow transition and found that it is governed by a number of factors, which include the method of gas introduction, pipe diameter, void fraction and the instability of void fraction waves [1–3]. The bubble size is suspected to be one key parameter affecting the critical void fraction at which the transition takes place [4]. Accurate measurement of the bubble size is, therefore, necessary to predict the transition between the two flow regimes.

Several methods are available at present to measure bubble size and void fraction in gas–liquid two-phase flows [5]. Popular ones include photography, gamma-ray absorption, ultrasonics, and optic fibre and resistivity probe methods. The latter two involve a needle-shaped probe, which can detect which of the two-phases is instantaneously present at the tip by using total internal reflection (optic fibre) or electrical conductivity. The electrical resistivity probe method is attractive for bubbly flow measurements because of its relative simplicity and wide applicability. It detects the passage of interfaces at the tip of each sensor, and uses this data to determine void fraction and bubble size and velocity [6,7,10]. The optic fibre has a faster response, but we have found commercial probes both expensive and too fragile to use in the large bubble column of our experiments.

Early versions involved only one needle, which gave two different signals depending upon whether the needle tip was in a bubble or in liquid. Hills [8] used a short needle with a single 90° bend and investigated the radial variation of gas hold-up in a vertical bubble column. Neal and Bankoff [9] also used the single 90° bent configuration and analysed bubble signals in terms of autocorrelation functions to obtain local values of gas fraction, bubble frequencies and bubble size. Serizawa et al. [7] developed the method further and presented a double-sensor probe for measuring local values of air–water bubbly flows. This probe had the advantage that it was capable of measuring bubble velocity from the time lag between a pair of upstream–downstream

* Corresponding author. Tel.: +44-115-951-4171; fax: +44-115-951-4115.
E-mail address: john.hills@nottingham.ac.uk (J.H. Hills).

1385-8947/01/$ – see front matter
PII: S1385-8947(00)00240-0

Table 1
Summary of probe configurations used by previous investigators

Authors	Resistivity probe			Configuration
	Material	Wire diameter (mm)	Probe separation (mm)	
Neal and Bankoff (1963) [9]	Stainless steel	0.75	–	Single 90° bent
Park et al. (1969) [20]	Kovar	1.0	9.5	Vertical
Rigby et al. (1970) [21]	Chromel–alumael	0.5	8.5	Vertical
Hills (1974) [8]	Tungsten	0.5	–	Single 90° bent
Serizawa et al. (1975) [7]	Stainless steel	0.2	5.0	90° bent
Hirama et al. (1975) [22]	Optical fibre	0.5	3.0	Horizontal
Kato et al. (1975) [23]	Platinum	2.0	–	Single 90° bent
Herringe and Davis (1976) [24]	Stainless steel	0.08	0.15–1.2	Vertical
Orazem et al. (1979) [14]	Platinum rhodium	2.0	3.0	Oblique
Ueyama et al. (1980) [15]	Platinum	0.5	4.3	Oblique
Lewis et al. (1983) [25]	Stainless steel	0.315	1.5	Vertical
Yasunishi et al. (1986) [16]	Platinum	0.25	3.0	Oblique
Choi et al. (1986) [26]	Chromel–alumel	0.25	3.0	Horizontal
Moujaes and Dougall (1987) [27]	Optical fibre	0.076	1.295	Vertical
Kocamustafaogullari and Wang (1991) [10]	Stainless steel	0.25	2.5	Vertical
Cheng (1997) [17]	Platinum	0.1	5.0	Vertical
Sanaullah et al. (1998) [13]	Stainless steel	0.112	2.0	Oblique

signals. It consisted of two identical electrically insulated needles placed side-by-side with their tips about 5.0 mm apart. Kocamustafagullari and Wang [10] recommended a 2.5 mm separation to account for possible bubble size and bubble velocity. A comprehensive list of previous probe designs is given in Table 1.

The problem with the two-point probe is the difficulty of matching the signals from the two needles which correspond to the same bubble, especially since bubbles do not always rise vertically, and often strike the probe with a glancing blow. One attempt to improve the situation is to use a five-point probe [11,12] with a leading needle surrounded by four needle tips in the same horizontal plane a few millimetre downstream of the central tip. The extra complexity involved has meant that these devices have not been used as much as the simpler two-point probe.

One of the major concerns with multiple probes is that the leading needle may interfere with the bubble, and so disturb the reading of the downstream needle(s). Calderbank's algorithm [11] for analysing data from his five-point probe rejected any bubble not seen simultaneously by three equi-spaced downstream needles, thus ensuring that only 'head-on' collisions, least likely to be affected, were analysed. This, however, meant that only a very small sample of the bubble population was included, raising doubts about whether the sample was representative.

The orientation of the resistivity probe needles is commonly either horizontal (perpendicular to the bubble path) or vertical. In the horizontal configuration, the ability of the probe to withstand the lateral drag of the fluid becomes an important factor; in the double needle probe, this leads to uncertainty about the exact vertical positions, and hence the separation, of the tips. However, with any double sensor probe, the two tips must be vertically one above the other,

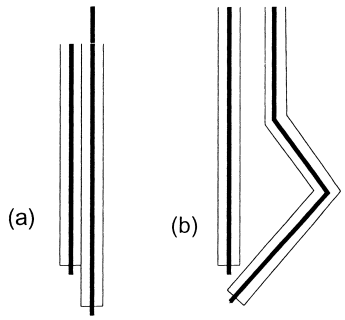

Fig. 1. Configurations of vertical two-needle probes.

which is impossible if both needles are vertical. Most recent workers have used two very fine needles touching each other, as shown in Fig. 1(a), to minimise this problem. Thus Cheng [17] made her needles from PTFE-coated wire with an outer diameter of 112 mm, assuming that this displacement would have minimal effect. However, the use of touching needles means that there is a danger of the liquid meniscus in the channel between them affecting the behaviour of the downstream needle tip. A common orientation in commercial two-point optic-fibre probes is to separate the two needles, but to bend the upstream one so that the two tips are aligned (Fig. 1(b)), but this raises the question as to whether the different orientations of the two probes influences the result.

A number of researchers in the past have used oblique probes [13–16] but very few have tried to investigate the impact of inclination on the measurements. In this work an attempt has been made to investigate the influence of probe inclination on measured bubble size and velocity. Two probes with different inclination angles have been constructed and measurements made under identical flow

conditions so that a direct comparison becomes possible. The probe design is discussed in detail in Section 2, and details of the experimental facility in Section 4.

The results from this study are compared with the data of Cheng [17] that were obtained with a vertical probe in the same column and under similar flow conditions. Results for bubble size, bubble frequency and interfacial area density for the three probes are discussed in Section 5.

2. Probe design

A schematic illustration of the resistivity probe is given in Fig. 2. It consists of two identical stainless steel wires (PTFE insulated) of 0.112 mm diameter. They are inclined at an angle so that their tips are aligned vertically with a distance of 5.0 mm between them, as this was the distance used by Cheng [17] in the vertical configuration. Too large a separation can introduce errors in the detected signals as multi-bubble contact may occur between two signals originating from the same bubble, whereas too small a separation will lead to errors in the estimation of velocity. Other design parameters depending upon the inclination angle are presented in Table 2.

The two sensors are electrically insulated from the probe body, except their tips, which are made by simply cutting the ends off the insulated wires. The other ends of the wires are soldered to two coaxial cables. The soldered connections are carefully electrically insulated using air dried insulating varnish and as an additional measure for safe insulation soldered connections are wrapped by heat shrinking plastic tubes. The other ends of the coaxial cables are connected to the bubble signal processor. The screens of these cables are joined to a lead whose other end touches the water in the column as the 'ground'. The signal processor mainly compares the resistance between the probe tip and the ground. A constant potential of 5 V DC is applied across each needle and the potential across a series resistor is amplified to provide the output signal.

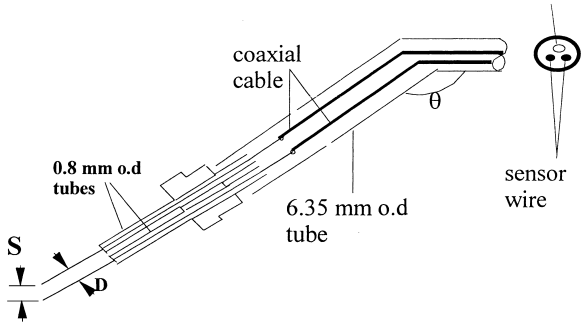

Fig. 2. A schematic illustration of an inclined dual-sensor resistivity probe.

Table 2
Resistivity probe design parameters (Fig. 3)[a]

θ (°)	S (mm)	D (mm)
90	5.0	2.0
110	5.0	1.72
145	5.0	2.86

[a] Probe wire material: stainless steel.

3. Data processing

The data acquisition system consists of a 12 bit (DT-2821) A/D converter operated by DATS_plus software loaded on a personal computer. The sampling frequency used is 25 kHz per sensor and a sampling duration of 60 s. The raw signals are not square-waves. This is due to the relatively slow drainage of liquid film formed around the sensor tip, which leads to a slow rise time as compared to the sharp fall time when the sensor re-enters the water. To obtain bubble properties, it is necessary to have data in terms of perfect square-waves with the rise and fall corresponding to the precise moment when the needle enters and leaves the gas phase. For this purpose, a suggestion of Serizawa [18] was adopted. The raw data is differentiated, and the moment when the value of the derivative crosses a certain threshold used as the interface contact time. This processing is done using the DATS_plus software to generate four data files, which contain the rise and fall time for upstream and downstream sensors. Full details are given by Cheng [17]. The data is then analysed via a discrimination program in Q-basic. The program checks that rise and fall signals on each sensor alternate, rejecting two successive rise or fall signals, and then attempts to match corresponding rise and fall signals from the two sensors for a given bubble. The algorithms for this are given by Cheng [17], and her discrimination parameters are also used in this work to make the results strictly comparable. Since the flow around the downstream needle is disturbed by the upstream probe, the downstream signals are less reliable, and results for void fraction and bubble frequency are based on the data obtained from the upstream probe.

The local void fraction α can be calculated from the sum of duration time t_g for bubbles at the upstream probe for the sample time T

$$\alpha = \frac{\Sigma t_g}{T} \tag{1}$$

Using the time lag between the signals for the two sensors and the vertical distance L between them, the velocity of the ith bubble, U_{Bi}, can be determined by the following equation:

$$U_{Bi} = \frac{L}{t_{di}} \tag{2}$$

where the average displacement time of liquid–gas interface and gas–liquid interface for a bubble travelling between the two sensors is given as

$$t_{di} = 0.5(t_{dri} - t_{uri}) + 0.5(t_{dfi} - t_{ufi}) \tag{3}$$

where subscript 'd' and 'u' corresponds to downstream and upstream, respectively, and 'r' and 'f' corresponds to rise and fall signals, respectively. The bubble chord length L_{Bi} is then obtained as

$$L_{Bi} = U_{Bi}(t_{uri} - t_{ufi}) \tag{4}$$

where the upstream contact time is used, as explained above, for its greater reliability.

Estimating bubble size distribution from the bubble chord length distribution is not easy, and even estimating the mean bubble size and velocity is not without problems. Since the probe is more likely to see a large bubble than a small one, complicated weighting factors are needed, but as the purpose of this work is merely to study the effect of probe orientation, we have used a simple number mean velocity and chord length. However, a Sauter mean bubble diameter can be obtained from an equation due to Kataoka et al. [19] for interfacial area concentration

$$\overline{a_i} = \frac{4N_t\{\overline{1/|U_{Bz}|}\}}{1 - \cot\frac{1}{2}\theta_0 \ln(\cos\frac{1}{2}\theta_0) - \tan\frac{1}{2}\theta_0 \ln(\sin\frac{1}{2}\theta_0)} \tag{5}$$

where N_t is the bubble frequency.

The equation assumes that bubbles are spherical and strike the probe while moving at an angle θ to the vertical with θ uniformly distributed in the range $0 \leq \theta \leq \theta_0$. The angle θ_0 can be estimated in terms of the measured mean bubble velocity and its standard deviation by assuming the velocity

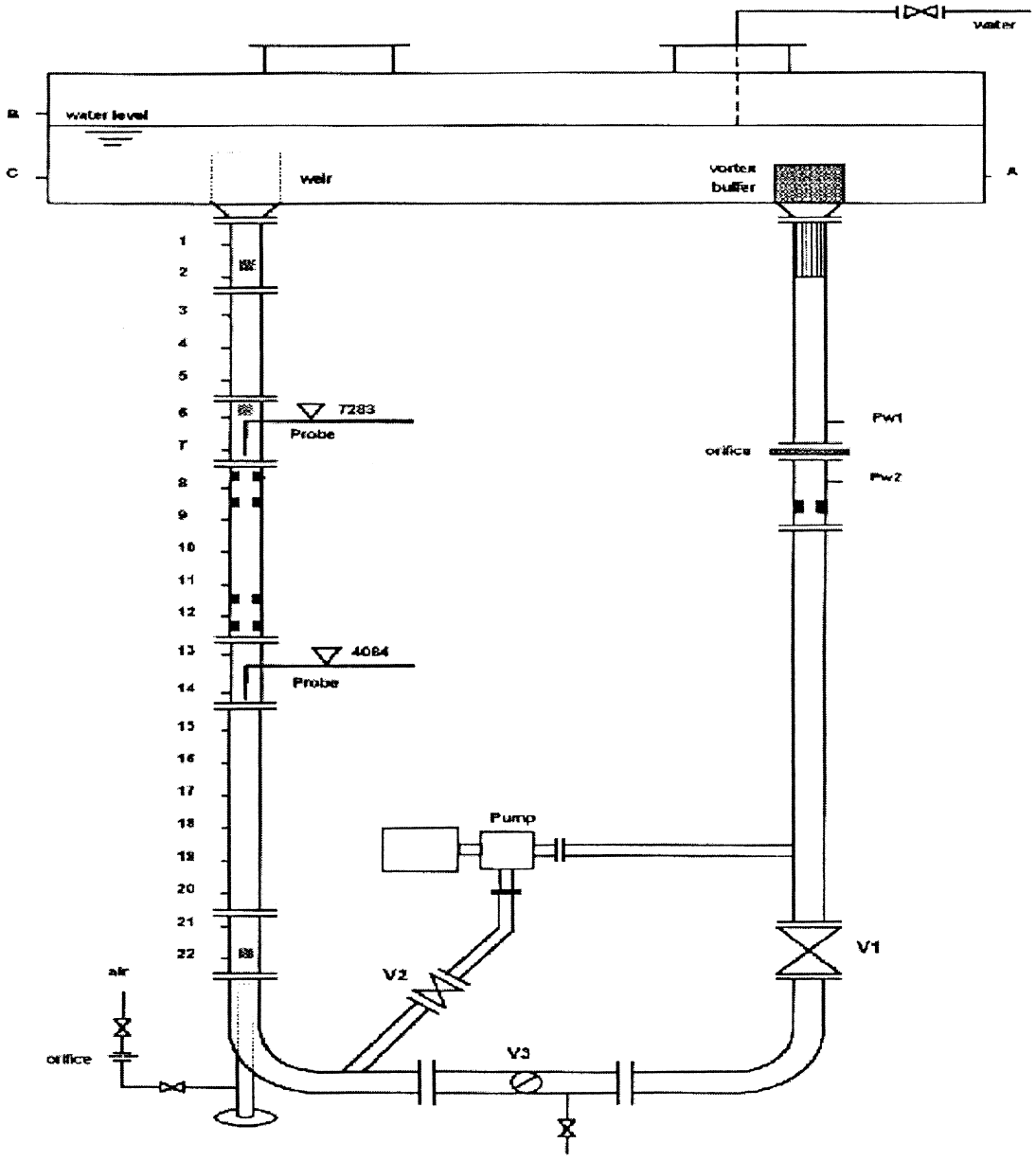

Fig. 3. A schematic layout of the experimental facility.

variations are isotropic [19]. This leads to the relation

$$\frac{\sin 2\theta_0}{2\theta_0} = \frac{1 - (\sigma_z^2/|\bar{U}_{Bz}|^2)}{1 + 3(\sigma_z^2/|\bar{U}_{Bz}|^2)} \quad (6)$$

Interfacial area can then be used to estimate the Sauter mean diameter, using

$$d_S = \frac{6\alpha}{\overline{a_i}} \quad (7)$$

4. Experimental facility

The schematic diagram of the rig is shown in Fig. 3. It consists of a 150 mm internal diameter column with a liquid circulating pump and a swirl reducing baffle. Five transparent sections have been provided to observe the flow patterns and the air entrainment in the column. The disengaging tank is located above the riser and has two 150 mm air vents and an overflow weir of 450 mm diameter. The transparent measuring section is located at a height of 4.0 m above the gas injector. Pressure tappings allow pressure readings at 450 mm intervals along the flow column. Air is fed directly from the 7 bar air main via an orifice plate and a needle valve to a central 51 mm pipe fitted with a sparger cap having 60 mm × 1 mm holes in the vertical cylinder. Filtered tap water was provided on a daily basis for this experiment. The water circulation rate was measured by an orifice plate and controlled by adjusting the butterfly valve in the bottom of the column as shown in Fig. 4.

5. Results and discussion

The experimental measurements were taken at a particular flow condition where the superficial liquid and gas velocities were fixed at 0.64 and 0.096 m/s, respectively. These flow conditions were chosen to make a direct comparison of the data from this experiment with those of Cheng [17] who conducted a study on the same flow column using a vertical resistivity probe. Visual and photographic observations at these flow conditions confirmed the existence of discrete bubbly flow in the column. No liquid circulation was observed near the walls, instead the bubble seems to migrate towards the centre of the pipe. This observation was confirmed by the void fraction measurements at various radial positions as will be discussed later in this section.

As mentioned in Section 2, two inclined probes with inclination angles of 110° and 145° were developed. Before investigating the impact of probe inclination on various measurements, the performance of the probes was monitored. This was achieved by comparing the results obtained from these probes with those obtained by Cheng [17] for a vertical probe under similar flow conditions. Experimental results for bubble frequency, local void fraction, mean bubble chord length and mean bubble velocity were examined and are presented in Fig. 4 for the 110° probe compared to Cheng's 90° (vertical) one. All four graphs show similar radial variations for the results from the two probes with pronounced central peaks for frequency (Fig. 4(a)) and void fraction (Fig. 4(b)). The two void fraction peaks are almost identical, whereas the vertical probe finds a somewhat higher

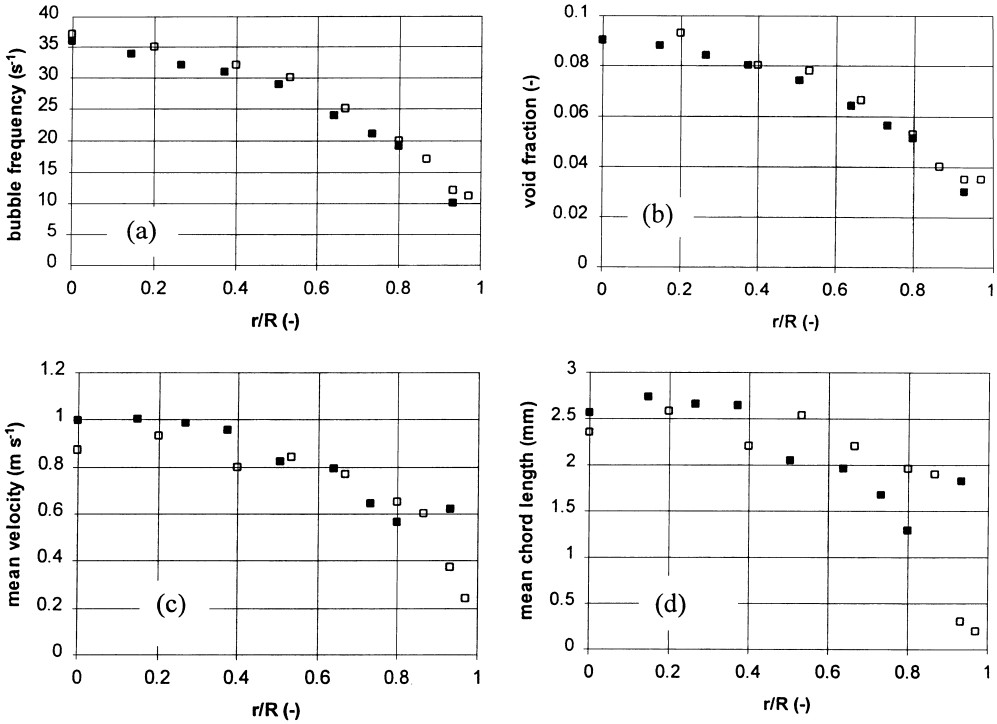

Fig. 4. Radial variation of: (a) bubble frequency; (b) void fraction; (c) bubble velocity; (d) mean chord length. Probe angle: (□): 90°; (■): 110°.

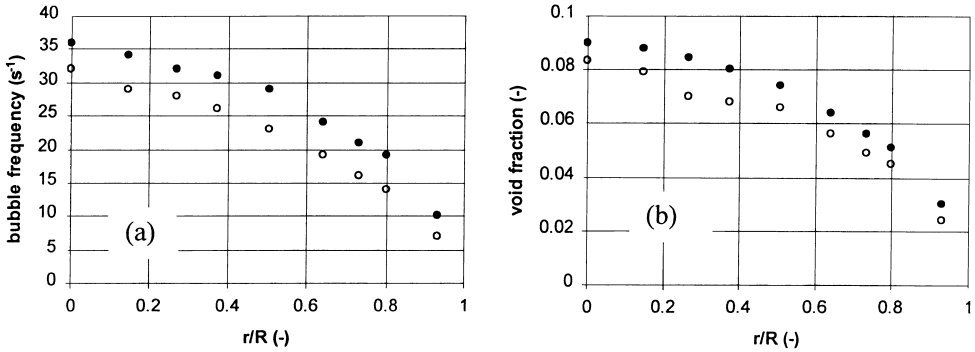

Fig. 5. Comparison of results from upstream (●) and downstream (○) needles of the 110° probe. (a) Bubble frequency; (b) void fraction.

frequency, which is odd as both measurements were made on the upstream needle. Fig. 4(c) gives the radial variation of the bubble mean velocity for the two probes. Again, both curves follow similar trends, but data for the 110° inclined probe lie on a somewhat smoother curve, and also show an odd increase near to the column wall. We are unable to explain this apparent increase which, from Eq. (4), leads to a corresponding apparent increase in mean chord length in Fig. 4(d). Apart from this near-wall point, the data from the 110° inclined probe in Fig. 4(d) are again on a smoother curve, and they also do not show the unexpected off-centre peak in chord length given by the vertical probe.

Comparing the bubble frequency and void fraction measurements from the two needles highlights any interference between them. This is shown in Fig. 5 for the 110° inclined probe, and it can be seen that the downstream needle sees fewer bubbles and records lower void fractions. The difference between the two measurements is relatively higher in the central region of the column and lower towards the walls. Similar observations were obtained for the other two probe angles. The main reason for this discrepancy is the hydrodynamic resistance experienced by a bubble as it passes the upstream needle. This leads the bubbles to move away from the downstream probe causing lower values of bubble frequency for the downstream probe as compared to those

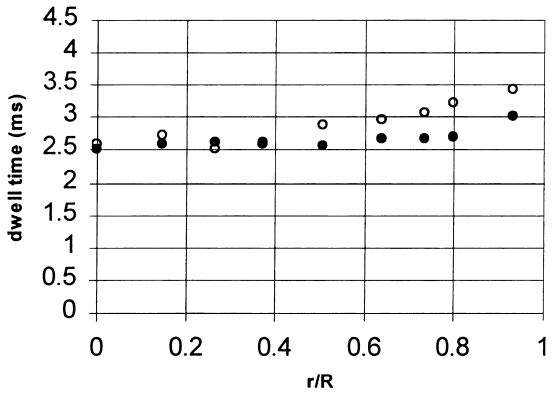

Fig. 6. Calculated mean dwell time of upstream (●) and downstream (○) needle tips of the 110° probe.

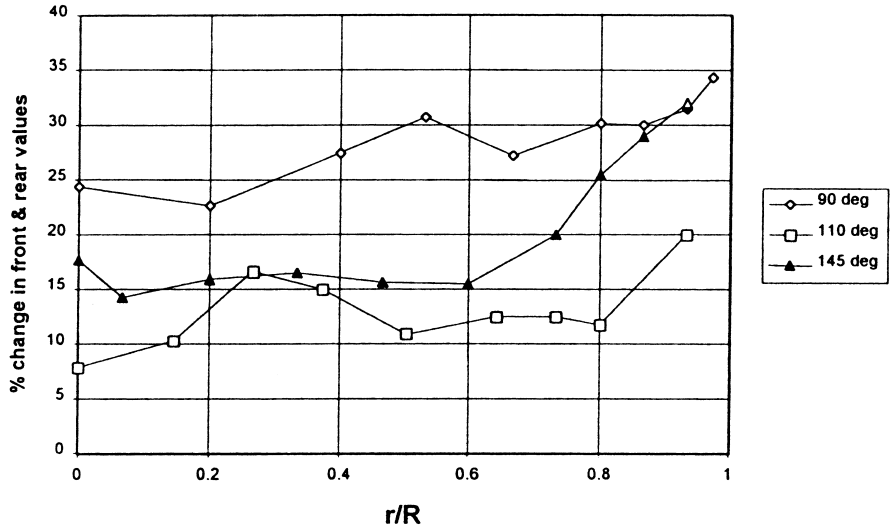

Fig. 7. Percentage change in the void fraction for three inclined probes.

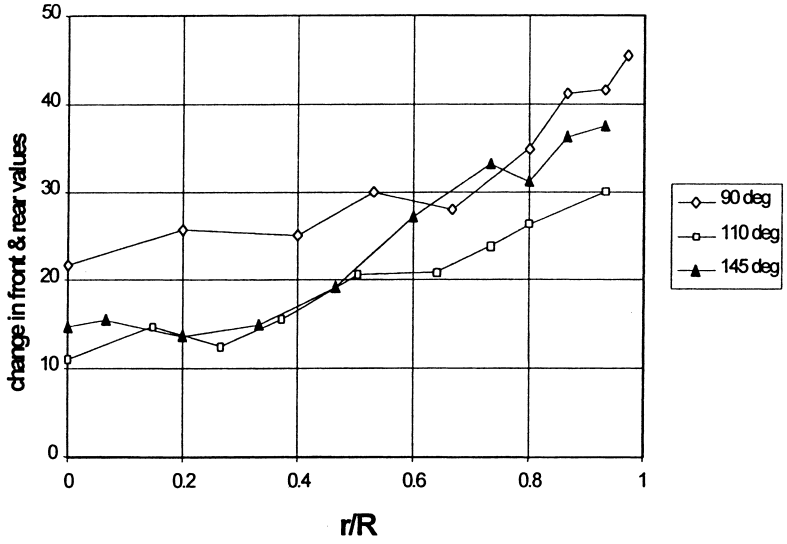

Fig. 8. Percentage change in the bubble frequency for three inclined probes.

obtained for the upstream probe as shown in Fig. 5(a). The reduced number of bubbles hitting the downstream probe is also the major factor in the lower void fraction recorded there. This can be seen in Fig. 6, which plots the ratio of void fraction to frequency, which gives the dwell time, or the average time a bubble spends in contact with the probe. It can be seen that, in the centre of the column the dwell time is the same for each needle and independent of position. It rises somewhat towards the column wall for the upstream needle, and significantly more for the downstream one. This latter result is hard to explain, since the 'pushing aside' mechanism described above ought to make the chord length, and hence the dwell time shorter for the second needle, but it occurs to a similar extent in all three probes.

The percentage change (i.e. ((front − rear)/front) × 100) in the void fraction and the bubble frequency for the upstream and downstream probe needles is shown in Figs. 7 and 8. The effect of probe inclination is remarkably high for both the local void fraction and the bubble frequency. It can be seen that for the vertical probe (90°), percentage change in the upstream and downstream bubble frequency values is the highest. It decreases as the inclination angle is changed from 90° to 110° but increases again for the 145° inclined probe as can be seen in Fig. 8. Fig. 7 shows a similar pattern for the percentage change in void fraction. It must be noted that the hydrodynamic resistance is a maximum for the vertical probe, reducing as the probe changes its position from vertical to horizontal but at the same time the probe needles become more unstable [19]. The probe

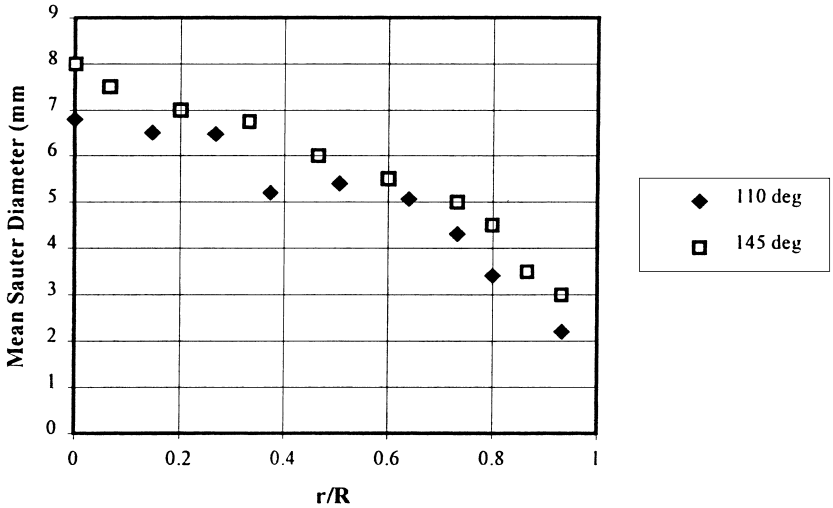

Fig. 9. Bubble size measurements for two inclined probes.

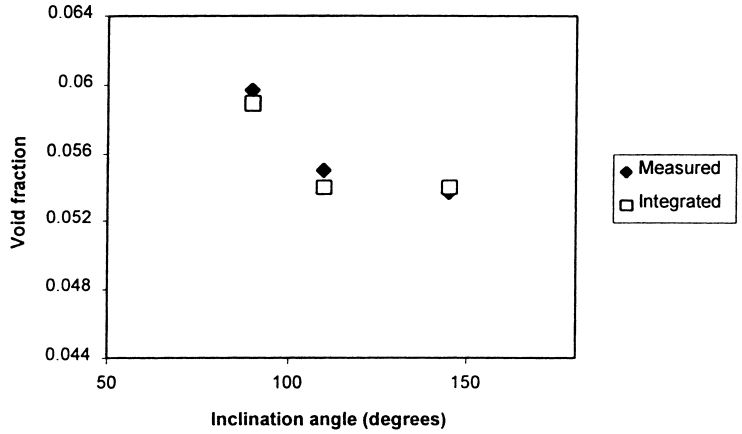

Fig. 10. Comparison of measured and integrated void fraction.

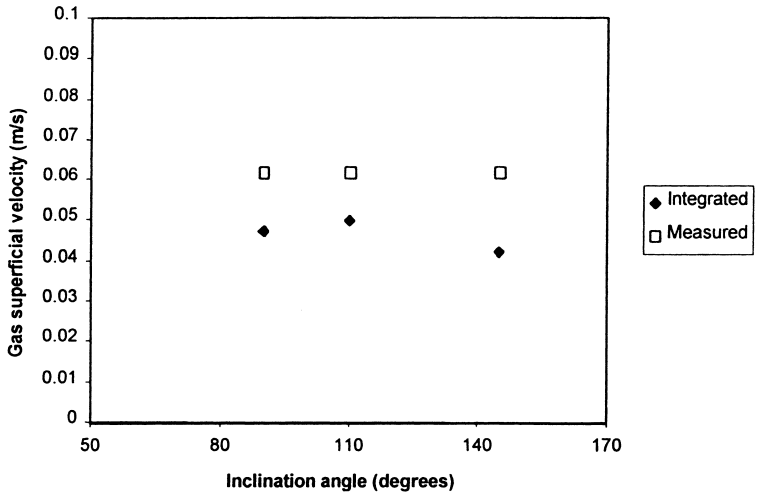

Fig. 11. Comparison of measured and integrated gas superficial velocity.

inclined at 110° finds the best compromise between two factors and indicates the minimum change in the upstream and the downstream values as compared to those obtained from the probes inclined at 90° and 145°.

Ideally, probes inclined at the three angles should give consistent results for bubble size. Fig. 9 shows the comparative study of bubble size. It can be seen that probes inclined at 110° and 145° gave almost identical radial variation of bubble size. However, the 90° probe data from Cheng [17] cannot be presented here for comparison as it seems that Cheng made some error in the calculation of interfacial area density that has led to unbelievably high values of bubble mean sauter diameter. Since her bubble frequency and velocity data are very similar to ours, they should give similar results when substituted in Eq. (5).

The accuracy of the data from our two inclined probes (110° and 145°) has also been checked by comparing the integrated void fraction and gas superficial velocity (= void fraction × bubble velocity) against directly measured values in the column. Cheng made similar calculations with her vertical probe data, and Figs. 10 and 11 show the results as a function of probe inclination. A good agreement was found in the void fraction whereas the measured values for the gas superficial velocity were relatively higher at all angles. This could be because the number mean velocity was used in the calculation and multiplied by the time mean void fraction. The correct calculation would be to sum the products of all individual bubble velocities and their dwell times and divide this by the elapsed time, but the fact that the velocity of a bubble can only be found when both needles are struck makes this impossible, since not all bubbles strike both needles.

6. Conclusions

Three inclined resistivity probes have been developed to measure bubble size, bubble frequency, local void fraction and interfacial area density concentration in a discrete bubbly flow. The impact of inclination on these measurements

has been studied. While the effect on the calculated parameters is small, there is a significant effect on the interaction between the two needles, as shown by calculating bubble frequency or void fraction from the upstream or the downstream needle. In this study among the three probes inclined at 90°, 110° and 145°, the 110° inclined probe showed the smallest difference between the two needles, which should make its results the most reliable. The accuracy of the probes was also checked by comparing the calculated values of the void fraction and the gas superficial velocities with those determined manometrically. A good agreement was found between the measured and the integrated values.

References

[1] N.N. Clark, R.L.C. Flemmer, The bubble to slug flow transitions in gas–liquid upflow and downflow, J. Pipelines 5 (1985) 53–65.

[2] A. Ohnuki, H. Akimoto, An experimental study on developing air water two-phase flow along a large vertical pipe: effect of air injection method, Int. J. Multiphase Flow 22 (6) (1996) 1143–1154.

[3] C.H. Song, H.C. No, M.K. Chung, Investigation of bubble flow developments and its transition based on the instability of void fraction waves, Int. J. Multiphase Flow 21 (3) (1995) 381–404.

[4] T.J. Liu, The effect of bubble size on void fraction distribution in a vertical channel, in: Proceedings of the International Conference on Multiphase Flow, ICMF'91, Tsukuba, September 24–27, Japan, 1991, pp. 453–457.

[5] G.F. Hewitt, Measurement of the Two Phase Flow Parameters, Academic Press, London, 1978.

[6] J.M. Delhaye, Two phase pipe flow, Int. Chem. Eng. 23 (3) (1983) 395–410.

[7] A. Serizawa, I. Kataoka, I. Michiyoshi, Turbulence structure of air–water bubbly flow. 1. Measuring techniques, Int. J. Multiphase Flow 2 (1975) 221–223.

[8] J.H. Hills, Radial non-uniformity of velocity and voidage in a bubble column, Trans. Inst. Chem. Engrs 52 (1974) 1.

[9] L.G. Neal, S.G. Bankoff, A high resolution resistivity probe for determination of local void properties in gas–liquid flow, AIChE J. 9 (4) (1963) 490–494.

[10] G. Kocamustafaogullari, Z. Wang, An experimental study on local interfacial parameters in a horizontal bubbly two-phase flow, Int. J. Multiphase Flow 17 (5) (1991) 553–572.

[11] J.M. Burgess, P.H. Calderbank, The measurement of bubble parameters in two-phase dispersions. I. The development of an improved probe technique, Chem. Eng. Sci. 30 (1975) 743–750.

[12] J. Buchholz, R. Steinemann, Application of an electrical conductivity microprobe for the characterisation of bubble behaviour in gas–liquid bubble flow, Part. Charact. 1 (1984).

[13] K. Sanaullah, S.H. Zaidi, J.H. Hills, Use of dual sensor inclined resistivity probe in novel applications, in: Proceedings of the Third International Conference on Multiphase Flow, ICMF'98, Lyon, France, June 8–12, 1998.

[14] M.E. Orazem, L.T. Fan, L.E. Ericson, Biotechnol. Bioeng. 21 (1979) 1579.

[15] K. Ueyama, S. Morooka, K. Koide, H. Kaji, T. Miyauchi, Ind. Eng. Chem. Proc. Des. Dev. 19 (1980) 592.

[16] A. Yasunishi, M. Fukuma, K. Muroyama, Measurement of behaviour of gas bubbles and gas hold-up in a slurry bubble column by a dual electroresistivity probe method, J. Chem. Eng. 19 (4) (1986) 444–449.

[17] H. Cheng, The bubble-to-slug flow pattern transition in vertical columns, Ph.D. Thesis, Department of Chemical Engineering, University of Nottingham, UK, 1997.

[18] A. Serizawa, 1994, personal communication.

[19] I. Kataoka, M. Ishii, A. Serizawa, Local formulation and measurements of interfacial area concentration in two-phase flow, Int. J. Multiphase Flow 12 (4) (1986) 505–529.

[20] W.H. Park, K.W. Kang, C.E. Capes, G.L. Osberg, The properties of bubbles in fluidised beds of conducting particles as measured by an electro-resistivity probe, Chem. Eng. Sci. 24 (1969) 851–856.

[21] G.R. Rigby, G.P.V. Blockland, W.H. Park, C.E. Capes, Properties of bubbles in three phase fluidised beds as measured by an electro-resistivity probe, Chem. Eng. Sci. 25 (1970) 1729–1741.

[22] T. Hirama, M. Ishida, T. Shirai, Kagaku Kogaku Ronbunshu 1 (1975) 272.

[23] Y. Kato, M. Nishinaka, S. Morooka, Kagaku Kogaku Ronbunshu 1 (1975) 530.

[24] R.A. Herringe, M.R. Davis, Structural development of gas–liquid mixture flows, J. Fluid Mech. 73 (1976) 97–123.

[25] D.A. Lewis, J.F. Davidson, Chem. Eng. Sci. 38 (1983) 161.

[26] K.H. Choi, J.W. Kim, W.K. Lee, Korean J. Chem. Eng. 3 (1986) 127.

[27] S. Moujaes, R.S. Dougall, Can. J. Chem. Eng. 65 (1987) 705.